JOURNAL OF BONE AND MINERAL RESEARCH
Volume 8, Number 1, 1993
Mary Ann Liebert, Inc., Publishers

# Physicochemical Effects of Acidosis on Bone Calcium Flux and Surface Ion Composition

DAVID A. BUSHINSKY,[1] WENDY WOLBACH,[2] NELSON E. SESSLER,[1]
RADION MOGILEVSKY,[2] and RICCARDO LEVI-SETTI[2]

## ABSTRACT

**Net calcium flux ($J_{Ca}$) from bone in vitro is pH dependent. When pH falls below 7.40, through a reduction in [$HCO_3^-$], there is both physicochemical and cell-mediated $J_{Ca}$. To characterize the physicochemical effect of acidosis on bone we inhibited the bone-resorbing cells (osteoclasts) with the specific inhibitor calcitonin and studied the effect of acidosis on $J_{Ca}$ and bone ion composition using an analytic high-resolution scanning ion microprobe. Neonatal mouse calvariae were cultured for 48 h in physiologically neutral pH medium (Ntl, pH = 7.41, [$HCO_3^-$] = 25 nM) or in medium that modeled metabolic acidosis (Met, pH = 7.10, [$HCO_3^-$] = 12), each with or without calcitonin (CT, $3 \times 10^{-9}$ M). There was net calcium efflux in Ntl ($J_{Ca}$ = 631 ± 36 nmol per bone per 48 h), which increased in Met (1019 ± 53, $p < 0.01$); CT inhibited $J_{Ca}$ in Ntl (−54 ± 11, $p < 0.01$ versus Ntl), which increased in Met (197 ± 15, $p < 0.01$ versus Ntl + CT). In the presence of CT the increase in $J_{Ca}$ in Met versus Ntl represents physicochemical bone dissolution. The Ntl bone surface (~2 nm in depth) was rich in Na compared to Ca (Na/Ca = 11.9, counts/s of detected secondary ions), which fell in Met (Na/Ca = 6.0, $p < 0.05$); CT caused a further reduction of Na/Ca (3.1, $p < 0.01$ versus Ntl and versus Met), which was not altered in Met (2.6, $p > 0.05$ versus Ntl + CT). The subsurface of the Ntl bone, eroded to a depth of ≅100 nm with the microprobe, was also rich in Na/Ca (11.0), which fell in Met (4.1, $p < 0.05$); CT caused a further fall in Na/Ca (3.8, $p < 0.01$ versus Ntl), which again was not altered in Met (3.5, $p > 0.05$ versus Ntl + CT). Acidosis causes a release of bone Ca and a fall in the ratio of bone Na/Ca, indicating a greater release of Na. Inhibition of osteoclastic function with calcitonin causes an influx of Ca to bone and a marked fall in bone Na/Ca, indicating little change in Na. Acidosis plus calcitonin causes Ca release with no change in Na/Ca, indicating that physicochemical bone mineral dissolution causes relatively equal Ca and Na release. Thus, the cell-mediated effect of acidosis-induced bone resorption appears responsible for the excess Na efflux.**

## INTRODUCTION

METABOLIC ACIDOSIS induces the release of bone mineral in vivo[1-4] and in vitro.[5-15] In vivo there is increased urine calcium excretion without a significant increase in intestinal calcium absorption, resulting in a negative net calcium balance.[1,4] Because the vast majority of body calcium is contained within the bone mineral, the negative calcium balance implies bone mineral dissolution,[16,17] and animals acidified with oral ammonium chloride have depleted bone mineral stores.[3,18]

In vitro acidosis produces calcium release through both physicochemical and cell-mediated mechanisms.[6-15] Over a short time interval (3 h), the calcium efflux is mediated through physicochemical mechanisms; the cellular component of calcium flux appears independent of medium pH during this acute time frame.[11] Over longer time intervals (greater than 24 h), there is net calcium efflux from bone that is due to cell-mediated mechanisms in addition to physicochemical dissolution.[12] Acidosis stimulates the bone-resorbing cells, the osteoclasts, and inhibits the bone-forming cells, the osteoblasts.[14] The net calcium efflux

[1]Nephrology Unit, University of Rochester School of Medicine and Dentistry, Rochester, New York.
[2]Department of Physics, Enrico Fermi Institute, University of Chicago, Illinois.

during acidosis is due to an increase in unidirectional calcium efflux[15] causing a loss of bone carbonated apatite.[6] During both short and longer duration studies the calcium efflux is greater when the medium is acidified by decreasing the concentration of bicarbonate (a model of metabolic acidosis) compared to increasing the partial pressure of carbon dioxide (a model of respiratory acidosis).[7,12,13,15]

Using an analytic high-resolution scanning ion microprobe we have found that the surface of bone is rich in sodium compared to calcium.[10,13,19-21] Acidosis produced by lowering the concentration of medium bicarbonate produces a marked fall in the surface sodium relative to calcium, in addition to increasing net calcium efflux.[10,13] These findings indicate that acidosis produces a greater loss of bone sodium than calcium. However, the relative contributions of physicochemical mineral dissolution and cell-mediated resorption to calcium and sodium movement could not be determined in these studies.

To separate the physicochemical from cell-mediated effects of acidosis on sodium and calcium release from the bone mineral, we cultured neonatal mouse calvariae with the specific osteoclastic inhibitor calcitonin and examined the bone surface with a high-resolution scanning ion microprobe utilizing secondary ion mass spectroscopy. We found that acidosis-mediated physicochemical bone mineral dissolution produces approximately equal sodium and calcium release. Thus, the excess sodium release in response to acidosis from bone with functioning osteoclasts appears due to cell-mediated mechanisms.

## MATERIALS AND METHODS

### *Culture procedures*

Neonatal (4–6 days old) CD-1 mice (Charles River, Portage, MI) were killed, their calvariae removed by dissection, and the adherent cartilaginous material trimmed.[6-15,19-21] Exactly 2.8 ml culture medium (Dulbecco's modified Eagle's medium with 4.5 g/liter of glucose; Whittaker M.A. Bioproducts, Walkersville, MD) containing heat-inactivated (1 h at 56°C) horse serum (15%), Na heparin (10 U/ml), and penicillin K (100 U/ml), was preincubated at a fixed chosen $P_{CO_2}$, 37°C, for 3 h in 35 mm Petri dishes; 1 ml was then removed to determine preincubation medium pH, $P_{CO_2}$, and calcium and sodium concentrations, and two calvariae were placed in each dish on a stainless steel wire grid. Total bone content in each culture dish was controlled by using pups that were the same age and size, by using a standardized dissection procedure, and by placing two bones in each dish. Experimental and control cultures were performed in parallel and in random order. Bones were incubated for 48 h at 37°C, at which time a second sample of culture medium was obtained and similarly analyzed. The incubator (Forma Scientific Model 3154, Marietta, OH) maintains a constant temperature (±0.02°C) and a constant $P_{CO_2}$ (±0.1%) at an ambient $O_2$ concentration of 21%.

### *Experimental groups*

Calvariae were studied in four groups: neutral pH (Ntl) and metabolic acidosis (Met), each with and without the osteoclastic inhibitor calcitonin (CT). In the Ntl groups, calvariae were cultured in unaltered medium at the physiologically neutral pH (pH ≅ 7.40) and at the physiologically normal $P_{CO_2}$ of 40 mm Hg. In the Met groups, medium pH was lowered to ≅7.10 by the addition of 0.01 ml concentrated HCl to lower the medium $HCO_3^-$ concentration. In the CT groups, $3 \times 10^{-9}$ M (final concentration salmon calcitonin (Bachem, Inc., Torrance, CA) was included in the medium.[14,22-26] This concentration of calcitonin (10 ng/ml) has been shown to maximally inhibit parathyroid hormone (PTH)-stimulated bone resorption in cultured neonatal mouse calvariae.[22,23] We previously utilized this concentration of calcitonin as an osteoclastic inhibitor.[14,24-26] In all cultures in which HCl was not added to the medium, 0.01 ml deionized, distilled water was added instead.

### *Scanning ion microprobe*

Calvariae were removed from the incubation medium, washed three times with deionized distilled water, rapidly frozen in an acetone and dry ice bath (−77°C), and then lyophilized while frozen until dry (at least 6 h).[10,13,19-21] The dry calvariae were mounted on aluminum supports with conductive glue and coated with a thin layer (~5 nm) of gold. This layer, which is rapidly sputtered away from the area being scanned, prevents artifact-inducing electrical charging.

The scanning ion microprobe (SIM) employs a 40 keV gallium beam focused to a spot 40 nm in diameter.[10,13,19-21,27-31] The beam is scanned across a sample surface in a controlled sequence, resulting in the emission of secondary electrons and atoms. These secondary particles originate within, and consequently carry information about, the most superficial 1-2 nm of the sample and can be used to generate images of the surface topography of a sample similar to those obtained using a scanning electron microscope. The sputtered particles that are emitted in an ionized state can also be collected and analyzed by secondary ion mass spectrometry (SIMS), a technique that separates the sputtered ions according to their mass-charge ratio.

Microanalysis of the calvariae by SIMS was performed in four distinct modes. In the imaging SIMS mode, the mass spectrometer is turned to transmit a single ion species while the probe is scanned over a square region of the sample surface. The result is a moniosotopic elemental distribution image, called a SIMS map. Because the mass-resolved counting rates during the image acquisition are recorded, these SIMS maps provide both a local quantitative record as well as a two-dimensional representation of the distribution of a particular element on the surface being scanned. In the nonimaging SIMS mode, the spectrometer is rapidly and sequentially retuned to filter several chosen ion species. At the same time, the probe is quickly scanned over a square area, so that the measured signals are secon-

dary ion intensities averaged over the entire field of view. Using this "peak-switching" technique, the relative concentrations of several elements can be acquired simultaneously from one area and at one sample depth. In the mass analysis mode, the spectrometer mass tuning can be systematically varied (as in a conventional mass spectrometer) to yield mass spectra. If the spectra data are corrected by element-dependent sensitivity factors, they provide quantitative relative abundance measurements for a given area of sample. In the final microanalysis mode, the gallium beam is used to sputter erode the surface, continually exposing deeper layers for analysis. As in the nonimaging SIMS mode, the peak-switching procedure is used to simultaneously analyze several ion species. As deeper layers are exposed, a depth profile can be created that characterizes composition as a function of depth. Erosion depth is estimated from the primary ion current, the average density of bone, the duration and area of the scan, and a secondary particle sputter yield of 10 that is typical of these materials.[10,13,19-21,27-31] Microanalysis using secondary ion emission has been used to map the distribution of elements on the surface and in the structure of mineralized and nonmineralized biologic tissues.[13,21,27,28,31-33] Previously we used this instrument to study the effects of low bicarbonate medium,[10] basal bone cell function,[19] and 1,25-dihydroxyvitamin $D_3$[20] to compare in vitro with in vivo $^{44}Ca$ labeling[21] and to compare the effects of in vitro models of metabolic and respiratory acidosis[13] on the relative concentration and distribution of ions in cultured neonatal mouse calvariae.

For SIMS analysis, the secondary ions emerging from the sample are transported through a high-transmission optical system containing an electrostatic energy analyzer and a radio frequency quadrupole mass spectrometer (mass resolution $\cong 0.1$ atomic mass units, AMU, measured at 40 AMU). The emergent mass-separated ions are accelerated (3000 V bias) for detection by a channel electron multiplier operated in pulse mode (each collected ion yields one digital pulse). Mass spectra are accumulated with a multichannel scaler that counts each detected ion by ramping the potential of the quadrupole spectrometer to scan a preselected mass region of the spectrum while the probe is scanning an area of arbitrary dimensions. The choice of the scanned area determines the depth over which the target composition is sampled for a given probe current and time. Elemental maps are obtained by displaying the indi-

TABLE 1. INITIAL MEDIUM pH, $P_{CO_2}$, AND $HCO_3^-$ CONCENTRATIONS[a]

| *Group* | n | *IpH* | *$IP_{CO_2}$ (mm Hg)* | *$I[HCO_3^-]$ (mEq/liter)* |
|---|---|---|---|---|
| Ntl | 8 | 7.406 ± 0.005 | 40.3 ± 0.4 | 25.0 ± 0.2 |
| Met | 8 | 7.101 ± 0.002[b] | 41.1 ± 0.2 | 12.2 ± 0.1[b] |
| Ntl + CT | 7 | 7.405 ± 0.003[c] | 40.5 ± 0.4 | 25.1 ± 0.1[c] |
| Met + CT | 7 | 7.094 ± 0.002[b,d] | 41.7 ± 0.3 | 12.2 ± 0.1[b,d] |

[a]All values are mean ± SEM; *n*, number of pairs of calvariae in each group; I, initial medium; $P_{CO_2}$, partial pressure of carbon dioxide; $[HCO_3^-]$, bicarbonate concentration. Ntl, calvariae incubated in unaltered medium at a physiologic pH, $P_{CO_2}$, and $HCO_3^-$; Met, calvariae incubated in reduced pH medium produced by a lowered $[HCO_3^-]$; CT, calvariae incubated in medium with $3 \times 10^{-9}$ M salmon calcitonin. All calvariae incubated for 48 h.

[b]Different from Ntl, $P < 0.05$.

[c]Different from Met, $P < 0.05$.

[d]Different from Ntl + CT, $P < 0.05$.

TABLE 2. INITIAL MEDIUM ION CONCENTRATIONS AND NET ION FLUXES[a]

| *Group* | *ICa (mM)* | *$J_{Ca}$ (nmol per bone per 48 h)* | *INa (mM)* | *$J_{Na}$ (nmol per bone per 48 h)* |
|---|---|---|---|---|
| Ntl | 1.82 ± 0.01 | 631 ± 35 | 150 ± 1 | 880 ± 177 |
| Met | 1.81 ± 0.01 | 1019 ± 53[b] | 149 ± 1 | 783 ± 85 |
| Ntl + CT | 1.81 ± 0.01 | −54 ± 11[b,c] | 150 ± 1 | 880 ± 143 |
| Met + CT | 1.81 ± 0.01 | 197 ± 15[b-d] | 149 ± 1 | 727 ± 102 |

[a]All values are means ± SEM; number of pairs of calvariae as in Table 1; I, initial medium concentration; Ca, calcium; Na, sodium; *J*, net ion flux; a positive number indicates ion movement from the bone into the medium. Ntl, calvariae incubated in unaltered medium at a physiologic pH, $P_{CO_2}$, and $HCO_3^-$; Met, calvariae incubated in reduced pH medium produced by a lowered $[HCO_3^-]$; CT, calvariae incubated in medium with $3 \times 10^{-9}$ M salmon calcitonin. All calvariae incubated for 48 h.

[b]Different from Ntl, $P < 0.05$.

[c]Different from Met, $P < 0.05$.

[d]Different from Ntl + CT, $P < 0.05$.

vidual detected pulses, suitably amplified and shaped, as counts on a video display. Images are recorded on Polaroid film in scans containing 512 × 512 picture elements encompassing a 40 × 40 $\mu m^2$ sample area. For the most abundant elements (Na and K), counting rates as high as $1.3 \times 10^4$ cps/pA of primary current were observed. In such cases statistically significant elemental images could be obtained in scan times of less than 100 s with probe currents of a few pA.

For each calvaria the surface and subsurface concentrations of $^{40}Ca$ and $^{23}Na$ were measured. From each experimental group, we randomly selected several intact calvariae, scanned them in their entirety, and made simultaneous ion determinations of $^{40}Ca$ and $^{23}Na$. The analyses were repeated on 10–22 representative uneroded areas (40 × 40 $\mu m^2$) of each bone. Surface data were recorded after the erosion of ~2 nm of material; this procedure ensured the removal of any superficial surface contamination, permitted the acquisition of highly reproducible surface measurements, and is consistent with our previously published studies.[10,13,19–21] Representative elemental images of $^{40}Ca$, $^{23}Na$, and $^{39}K$ were then made for each sample. Given the beam current of 40 pA and image acquisition time not exceeding 524 s, the depth of erosion for these topographic and elemental measurements never exceeded ~20 nm, which did not result in significant sample depletion because calvariae are thicker than 10 $\mu m$. Finally, the gallium beam was used to sputter erode the bone while the spectrometer was adjusted to filter, using the peak-switching capability of the instrument, the $^{40}Ca$ and $^{23}Na$ secondary ions. In this manner the relative subsurface concentrations of these ions were determined as a function of depth.

Correction methods similar to those that we previously reported[10,13,19–21,29] were applied to the observed mass-resolved counting rates to obtain secondary ion yields proportional to the elemental concentration in the sample. Corrections are necessary because of the species-dependent ionization probabilities of the emitted atoms. Relative to calcium taken as standard, the corrected yields for sodium were obtained by dividing the observed counting rates by the sensitivity factor 1.9 for apatites, assumed to apply to other bone crystals as well.

The total ion counts in a micrograph are a function not only of the emission properties of ions from a sample but also of the fraction of the field of view occupied by the sample, which in this case is a calvaria. Calvariae occasionally have physical holes and on cross section often do not occupy the entire scanned field of view even at the highest magnification used in these studies. In addition, the detected ion yields are dependent on the degree of sample surface roughness. Because of these considerations, we express our results in terms of the ratios of counts of sodium to calcium obtained for the same area of a sample.[10,13,19–21] Such ratios are independent of the fraction of the field of view occupied by the sample and of the surface topography.

### *Conventional measurements*

pH and $P_{CO_2}$ were measured with a blood gas analyzer (Radiometer Model ABL30, Copenhagen, Denmark). Medium $[HCO_3^-]$ was calculated from the pH and $P_{CO_2}$ using the Henderson-Hasselbalch equation.[6–10,12–15,20,21] Medium total calcium concentration was measured by automatic fluorometric titration (Calcette; Precision Systems, Sudbury, MA), which we have shown to give results similar to those obtained using atomic absorption spectroscopy.[11] Medium sodium concentration was measured by flame photometry (Instrumentation Laboratory Model 343, Lexington, MA).

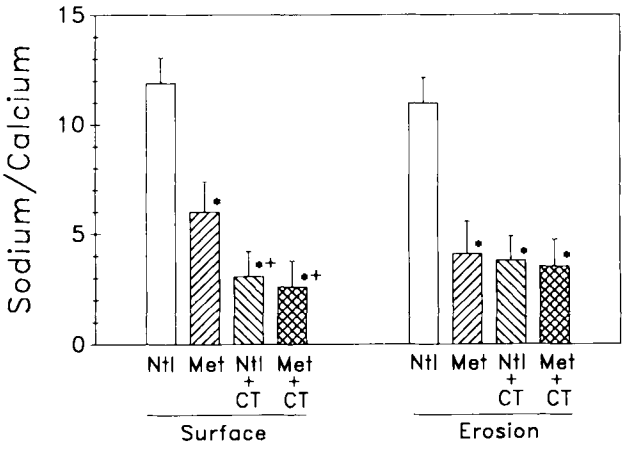


**FIG. 1.** Mean values and upper 95% confidence intervals are ratios of counts per second of detected secondary ions at the surface (~2 nm in depth) and eroded surface (~100 nm in depth) of cultured neonatal mouse calvariae. All calvariae were cultured for 48 h in physiologically neutral pH medium (Ntl, pH ≅ 7.41) or acid medium (Met, pH ≅ 7.10), with or without the osteoclastic inhibitor calcitonin (CT, $3 \times 10^{-9}$ M final concentration). Counts are corrected for the species-dependent ionization probabilities of sputtered ions and calculated as described in Materials and Methods. Upper 95% confidence intervals were calculated as in Materials and Methods. *Different from Ntl, same depth, $p < 0.05$; †different from Met, same depth, $p < 0.05$. At the surface the ratio of sodium to calcium was lower in Met than in Ntl; the ratio fell further with both Ntl + CT and Met + CT, which were not different from each other. At the eroded surface, compared to Ntl, the ratio of sodium to calcium was lower in Met, in Ntl + CT, and in Met + CT, which were not different from each other.

### *Flux calculations*

Net ion flux was calculated as $V_m$ ($ion_f$ − $ion_i$), where $V_m$ is the medium volume (1.8 ml) and $ion_f$ and $ion_i$ are the final and initial ion concentrations.[6–15,19–21] For all fluxes a positive value indicates movement of the ion from the bone into the medium and a negative value indicates movement from the medium into the bone. Fluxes are expressed as nanomoles per bone per 48 h.

### *Mean ion ratio calculations*

Mean ion ratios were calculated as the difference between the logarithm of the counts in the numerator and the logarithm of the counts in the denominator. The mean of

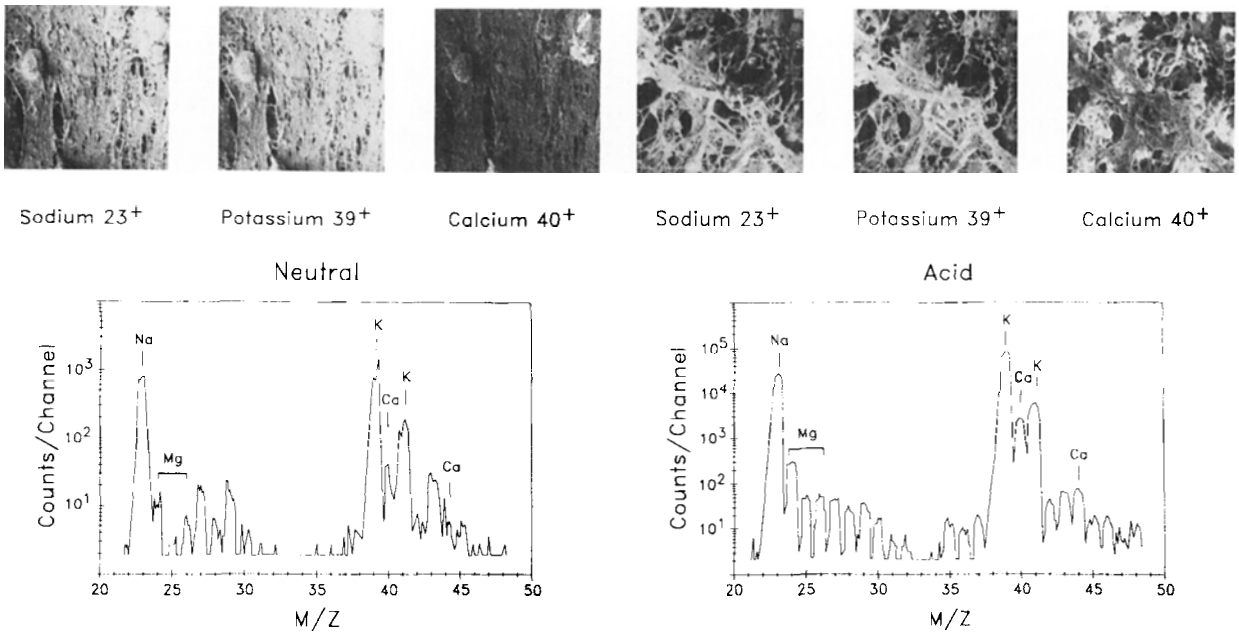


**FIG. 2.** Secondary ion mass spectrometry (SIMS) elemental distribution maps of sodium ($^{23}Na$), potassium ($^{39}K$), and calcium ($^{40}Ca$) and mass spectrum of the surface of a representative neonatal mouse calvaria after culture for 48 h in neutral pH (pH ≅ 7.41) medium. For sodium, potassium, and calcium, lighter areas indicate a greater abundance of the specific isotope compared with darker areas. Each micrograph is of the same area and is of similar magnification (40 μm square). Areas that are black in all three elemental maps appear to be physical holes or deep recesses in the surface. Mass spectra indicate that the abundance of calcium is less than that of sodium. Observed spectra were measured in 615 channels equally divided among mass 20–50 AMU. Counts per channel are counts per second of detected secondary ions uncorrected for species-dependent ionization probabilities. Relative to calcium as a standard, corrected yields for sodium are obtained by dividing their observed counting rates by a sensitivity factor of 1.9; *M/Z*, mass per unit charge.

**FIG. 3.** Secondary ion mass spectrometry (SIMS) elemental distribution maps of sodium ($^{23}Na$), potassium ($^{39}K$), and calcium ($^{40}Ca$) and mass spectrum of the surface of a representative neonatal mouse calvaria after culture for 48 h in acid pH (pH ≅ 7.10) medium. For sodium, potassium, and calcium, lighter areas indicate a greater abundance of the specific isotope compared with darker areas. Each micrograph is of the same area and is of similar magnification (40 μm square). Areas that are black in all three elemental maps appear to be physical holes or deep recesses in the surface. Mass spectra indicate that the abundance of calcium is less than that of sodium. Observed spectra were measured in 615 channels equally divided among mass 20–50 AMU. Counts per channel are counts per second of detected secondary ions uncorrected for species-dependent ionization probabilities. Relative to calcium as a standard, corrected yields for sodium are obtained by dividing their observed counting rates by a sensitivity factor of 1.9; *M/Z*, mass per unit charge.

the differences in each group was then obtained and analysis of variance calculated. Values expressed are the antilogarithm of the mean of the differences in each group plus or minus the upper and lower 95% confidence limits. The confidence limits were obtained by taking the means of the differences in each group and either adding, for the upper confidence limit, or subtracting, for the lower confidence limit, the product of 2.24 times the standard error of this mean and then calculating the antilogarithm of the resulting values. The number 2.24 is the *T* score for a one-tailed $p < 0.025$, so that 2.5% of the data lies above the upper confidence limit and 2.5% lies below the lower confidence limit.[14,19–21]

### *Statistics*

All tests of significance were calculated using analysis of variance (BMDP, University of California at Los Angeles, CA) on an IBM Personal System/2 computer (Model 90 XP486; IBM Corp., Armonk, NY). Values are expressed as mean ± standard error of the mean (SEM); $P < 0.05$ was considered significant.

## RESULTS

### *Initial medium pH, $P_{CO_2}$ and $[HCO_3^-]$*

Compared to Ntl, the initial medium pH and $[HCO_3^-]$ were reduced with Met (Table 1). Compared to Ntl + CT, the initial medium pH and $[HCO_3^-]$ were also reduced with Met + CT. There was no difference in initial medium pH or $[HCO_3^-]$ between Ntl and Ntl + CT or between Met and Met + CT. The initial medium $P_{CO_2}$ was not different in any group.

### *Initial medium ion concentrations and net ion fluxes*

There was no difference in initial medium Ca or Na in any group (Table 2). Compared to Ntl, there was a greater net Ca efflux with Met. With CT, there was net Ca influx

with Ntl + CT and a net Ca efflux with Met + CT that was greater than Ntl + CT but less than Met.

### *Effect of acidosis on surface ion composition*

At a depth of ~2 mm the surface of Ntl calvariae was rich in Na compared to Ca (Na/Ca = 11.9, + 13.7, −10.3 counts/s of detected secondary ions, mean, +, −, 95% confidence limit; Figs. 1 and 2). Compared to Ntl, the surface Na/Ca fell with Met (Na/Ca = 6.0, +8.3, −4.3, $p < 0.001$ versus Ntl; Figs. 1 and 3) and with Ntl + CT, Na/Ca fell further (Na/Ca = 3.1, +3.5, −2.7, $p < 0.001$ versus Ntl and versus Met; Figs. 1 and 4). However, compared to Ntl + CT, there was no further change in Na/Ca with Met + CT (Na/Ca = 2.6, +3.1, −2.2, $p > 0.05$ versus Ntl + CT; Figs. 1 and 5).

### *Effect of acidosis on subsurface ion composition*

At a depth of ~100 nm the subsurface of Ntl calvariae was also rich in Na compared to Ca (Na/Ca = 11.0, +12.9, −9.3; Fig. 1). Compared to Ntl, the subsurface Na/Ca fell with Met (Na/Ca = 4.1, +6.1, −2.7, $p < 0.001$ versus Ntl), as it did with Ntl + CT (Na/Ca = 3.8, +4.2, −3.4, $p < 0.001$ versus Ntl) and with Met + CT (Na/Ca = 3.5, +4.3, −2.9, $p < 0.001$ versus Ntl). There was no difference in subsurface Na/Ca with Met, Ntl + CT, or Met + CT ($p > 0.05$, all comparisons between Met, Ntl + CT, and Met + CT).

### *Ionic depth profiles*

Throughout the most superficial 5.5 nm in depth from the surface the ratio Na/Ca was lower in Met than in Ntl

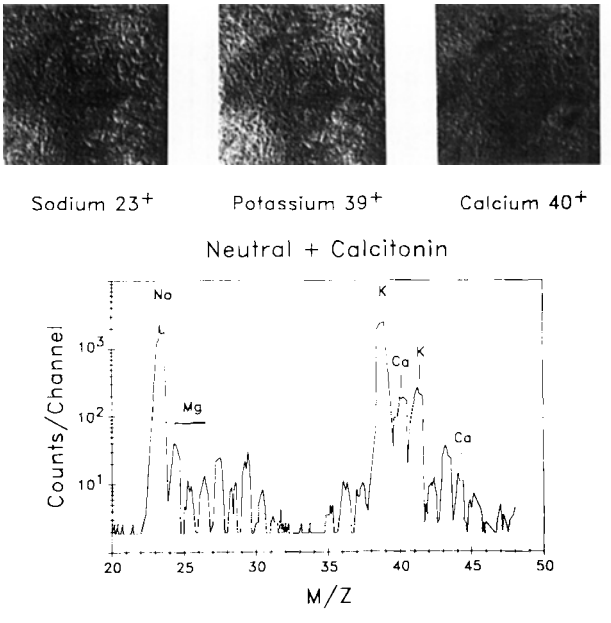


**FIG. 4.** Secondary ion mass spectrometry (SIMS) elemental distribution maps of sodium ($^{23}$Na), potassium ($^{39}$K), and calcium ($^{40}$Ca) and mass spectrum of the surface of a representative neonatal mouse calvaria after culture for 48 h in neutral pH (pH ≅ 7.41) medium with the osteoclastic inhibitor calcitonin ($3 \times 10^{-9}$ final concentration). For sodium, potassium, and calcium, lighter areas indicate a greater abundance of specific isotope compared with darker areas. Each micrograph is of the same area and is of similar magnification (40 μm square). Areas that are black in all three elemental maps appear to be physical holes or deep recesses in the surface. Mass spectra indicate that the abundance of calcium is less than that of sodium. Observed spectra were measured in 615 channels equally divided among mass 20–50 AMU. Counts per channel are counts per second of detected secondary ions uncorrected for species-dependent ionization probabilities. Relative to calcium as a standard, corrected yields for sodium are obtained by dividing their observed counting rates by a sensitivity factor of 1.9; *M/Z*, mass per unit charge.

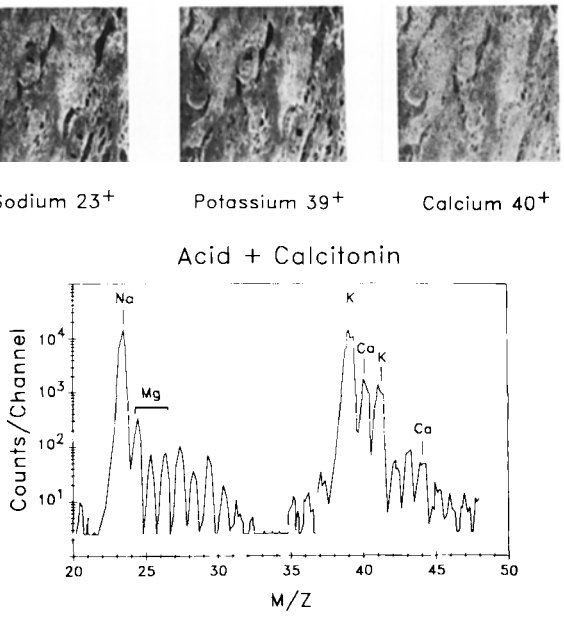


**FIG. 5.** Secondary ion mass spectrometry (SIMS) elemental distribution maps of sodium ($^{23}$Na), potassium ($^{39}$K), and calcium ($^{40}$Ca) and mass spectrum of the surface of a representative neonatal mouse calvaria after culture for 48 h in acid pH (pH ≅ 7.10) medium with the osteoclastic inhibitor calcitonin ($3 \times 10^{-9}$ final concentration). For sodium, potassium, and calcium, lighter areas indicate a greater abundance of specific isotope compared with darker areas. Each micrograph is of the same area and is of similar magnification (40 μm square). Areas that are black in all three elemental maps appear to be physical holes or deep recesses in the surface. Mass spectra indicate that the abundance of calcium is less than that of sodium. Observed spectra were measured in 615 channels equally divided among mass 20–50 AMU. Counts per channel are counts per second of detected secondary ions uncorrected for species-dependent ionization probabilities. Relative to calcium as a standard, corrected yields for sodium are obtained by dividing their observed counting rates by a sensitivity factor of 1.9; *M/Z*, mass per unit charge.

(Fig. 6). The ratio Na/Ca was still lower in Ntl + CT and in Met + CT, which were not different from each other at any depth.

Throughout the initial 125 nm in depth from the surface, the ratio Na/Ca continued to be lower in Met than in Ntl (Fig. 7). With increasing depth from the surface the ratio Na/Ca in Met + CT fell to levels not different from Ntl and Ntl + CT.

## DISCUSSION

After culture for 48 h in neutral pH medium the surface of neonatal mouse calvaria has abundant sodium relative to calcium. Incubation of calvariae in physiologically acid medium lowers the ratio of sodium to calcium and induces net calcium efflux from the mineral (Fig. 8), indicating that bone sodium must be leaving the mineral surface in excess of calcium. The inhibition of osteoclastic function with calcitonin lowers the rato of sodium to calcium and induces net calcium influx into the mineral (Fig. 8), indicating little change in bone sodium. When calcitonin-treated calvariae are incubated in acid medium, there is calcium efflux and no change in the ratio of sodium to calcium compared to calvariae treated with calcitonin in neutral medium (Fig. 8), indicating that calcium and sodium must be leaving the calvariae at this constant ratio in response to acid. Thus the excess sodium loss from calvariae incubated in acid medium without calcitonin appears due to cell-mediated resorption.

The fall in the ratio of surface sodium to calcium with acidosis is consistent with the hypothesis that protons induce the cell-mediated loss of sodium and, to a lesser extent, calcium from the bone surface. That the ratio of sodium to calcium does not change with acidosis in calcitonin-treated calvariae indicates that the excess sodium release is mediated by osteoclasts. Osteoclasts are known to secrete protons into the microenvironment between the cell and the mineral, which solubilizes the bone-carbonated apatite and induces mineral dissolution.[6,34] The carbonated apatite mineral phase is highly substituted with such ions as sodium,[6,35] and our data indicate that protons induce the release of bone sodium to an even greater extent than calcium through osteoclastic-mediated mechanisms. It is unclear why protons secreted by osteoclasts affect the bone mineral in a manner that is different from how protons affect the mineral directly. This difference may be related to the concomitant osteoclastic secretion of collagenase and proteases.[34] We and others have proposed that the calvarial surface in contact with the medium cannot be the carbonated apatite itself but rather may be an unmineralized matrix or "bone membrane."[19] It is perhaps this sodium-rich, calcium-poor, unmineralized matrix that is resorbed by the osteoclasts in response to acidosis and is not affected by the protons directly.

We would not have expected to detect changes in medium sodium concentration even after incubation in the acid medium. The ratio of bone surface sodium to calcium fell by approximately 50% after incubation in acid medium (Na/Ca = 11.9 counts per second of detected secondary ions in Ntl to 6.0 in Met) when an additional 0.4 mM calcium left the bone and entered the medium (change in medium calcium concentration in Ntl was 0.7 mM; change in medium calcium concentration in Met was 1.1 mM).

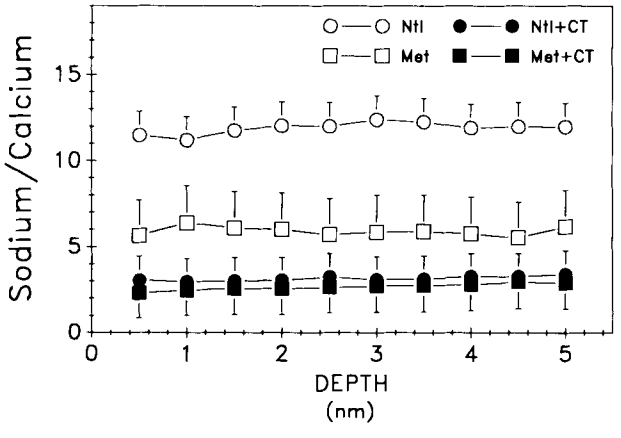


FIG. 6. Relationship between sodium/calcium and depth (0–0.5 nm) for neonatal mouse calvariae incubated for 48 h in neutral pH medium (open circles, $n$ = 22) or in acid pH medium (open squares, $n$ = 11) or with the osteoclastic inhibitor calcitonin ($3 \times 10^{-9}$ M final concentration) in neutral pH medium (closed circles, $n$ = 10) or in acid pH medium (closed squares, $n$ = 11). The superficial surface (0 depth) was eroded with the gallium beam toward the center of the bone. Values are the ratios of the counts per second of detected secondary ions corrected for species-dependent ionization probabilities of sputtered ions and calculated as described in Materials and Methods.

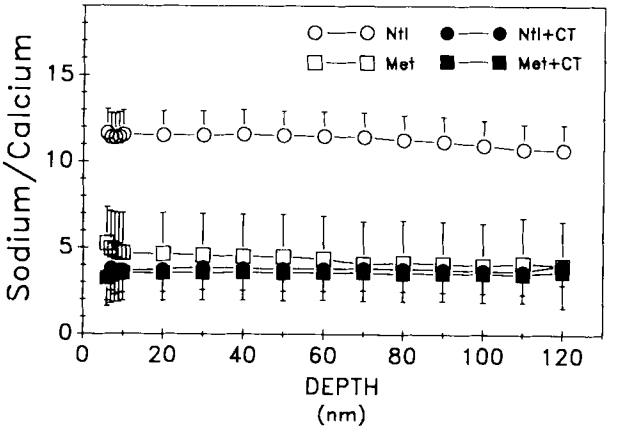


FIG. 7. Relationship between sodium/calcium and depth (6–120 nm) for neonatal mouse calvariae incubated for 48 h in neutral pH medium (open circles, $n$ = 22) or in acid pH medium (open squares, $n$ = 11) or with the osteoclastic inhibitor calcitonin ($3 \times 10^{-9}$ M final concentration) in neutral pH medium (closed circles, $n$ = 10) or in acid pH medium (closed squares, $n$ = 11). The superficial surface was eroded with the gallium beam toward the center of the bone. Values are the ratios of the counts per second of detected secondary ions corrected for species-dependent ionization probabilities of sputtered ions and calculated as described in Materials and Methods.

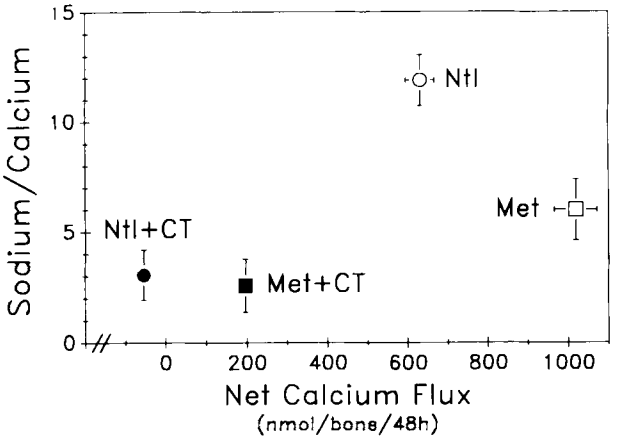


**FIG. 8.** Relationship between sodium/calcium and net calcium flux for neonatal mouse calvariae incubated for 48 h in neutral pH medium (circles) and acid pH medium (squares) with (closed symbols) and without (open symbols) the osteoclastic inhibitor calcitonin ($3 \times 10^{-9}$ M final concentration). Values for sodium/calcium are the ratios of the counts per second of detected secondary ions corrected for species-dependent ionization probabilities of sputtered ions and calculated as described in Materials and Methods. Net calcium flux is calculated as $V_m(Ca_f - Ca_i)$, where $V_m$ is the medium volume (1.8 ml) and $Ca_f$ and $Ca_i$ are the final and initial Ca concentrations. A positive value indicates movement of the ion from the bone into the medium, and a negative value indicates movement from the medium into the bone; values are expressed as nanomoles per bone per 48 h.

This implies that the sodium efflux might double, compared to calcium, to approximately 0.8 mM. This change in medium concentration would not easily be detected by the flame photometer because the baseline sodium concentration was 150 mM.

The loss of bone sodium and calcium during acidosis is consistent with in vivo observations in animals and humans. Rats have been shown to lose 7 mEq/kg of prelabeled bone $^{22}Na$ and dogs lose 6.6 mEq/kg of rib $^{24}Na$ after 5 h of metabolic acidosis.[36] Dogs infused with acid release sodium into the extracellular fluid.[37] When a human is given an acid load in the form of ammonium chloride, there is negative sodium balance before a negative calcium balance, implying an initial loss of bone sodium.[1]

Osteoclasts are responsible for cell-mediated bone resorption, and calcitonin is a specific inhibitor of osteoclastic function.[34,38] We do not believe that what we term physicochemical bone dissolution could be due to alterations in function of other cell types within the bone. Osteoblasts are responsible for laying down the unmineralized matrix, and we have shown that acidosis decreases osteoblastic collagen synthesis in vitro.[14] However, a decrease in osteoblastic matrix production would only decrease calcium influx into the matrix and could not, by itself, result in a net calcium efflux. No other cell types have been reported to be altered by acidosis.

We chose to utilize hydrochloric acid, not another mineral or organic acid, to produce an acid medium that replicates, as closely as possible, the acidosis induced by diarrhea, the most common form of metabolic acidosis found in vivo.[39] Diarrheal fluid has a high concentration of bicarbonate, and its loss results in a lowering of the extracellular fluid bicarbonate concentration. The addition of hydrochloric acid to the culture medium also lowers medium bicarbonate concentration without the addition of accompanying impermeable or organic anions. Further studies are needed to determine if acidosis produced by organic or other mineral acids has a similar effect on the bone mineral as acidosis produced by the addition of hydrochloric acid.

The ion ratios that we measured on the surface and eroded subsurface of the calvariae cultured in neutral medium are consistent with those we reported previously. We showed that this superficial bone surface is rich in sodium relative to calcium.[10,13,19-21] The presence of a large amount of sodium relative to calcium on the bone surface may represent a large fraction of unmineralized osteoid. However, this most superficial bone surface is in contact with the extracellular fluid and may well be the bone that first responds to changes in proton concentration. Previously we showed that there is a fall in the ratio of sodium to calcium with models of metabolic (decreased medium bicarbonate concentration) acidosis of 3 and 48 h in duration.[10,13] The ion flux data that we report in this study are consistent with those from our previous studies.[7,8,10-15,24] We showed that calvariae incubated in acid medium release more calcium than calvariae cultured in neutral pH medium[8-10,12-15] and that inhibiting osteoclastic function with calcitonin[24] or killing the bone cells[11] results in a net influx of calcium into the bone. In previous studies we were also not able to detect acidosis-induced changes in sodium flux.[10,13]

The net calcium efflux observed in the control experiments may be secondary to the effect of organic acids generated over 48 h by the calvariae. We previously showed that the medium pH in control cultures falls slightly during incubation.[7,8,12,15] Additionally, Stern et al. showed that some serum proteins, which may be concentrated from preparations of serum albumin, stimulate baseline calcium resorption.[40,41]

Thus physicochemical bone mineral dissolution results in the proportional loss of mineral calcium and sodium, whereas cell-mediated bone resorption results in the loss of excessive bone sodium relative to calcium. Neonatal mouse calvariae in culture respond to protons and calcium-regulating hormones, synthesize DNA and protein, and have functioning osteoblasts and osteoclasts as does human bone in vivo.[17] However, there are differences between calvariae and human bone: calvariae are neonatal woven bone compared with mostly mature cortical bone in humans, and in culture calvariae are not perfused by blood.[17] Thus it is not yet established whether these results obtained in vitro are applicable to human bone in vivo.

## ACKNOWLEDGMENTS

This study was supported by Grants AR 39906 and AM 33949 from the National Institutes of Health and by Grant DIR 9017112 from the National Science Foundation.

## REFERENCES


1. Lemann J Jr, Litzow JR, Lennon EJ 1966 The effects of chronic acid loads in normal man: Further evidence for the participation of bone mineral in the defense against chronic metabolic acidosis. J Clin Invest **45**:1608–1614.
2. Barzel US 1969 The effect of excessive acid feeding on bone. Calcif Tissue Res **4**:94–100.
3. Barzel US, Jowsey J 1969 The effects of chronic acid and alkali administration on bone turnover in adult rats. Clin Sci **36**:517–524.
4. Lemann J Jr, Litzow JR, Lennon EJ 1967 Studies of the mechanism by which chronic metabolic acidosis augments urinary calcium excretion in man. J Clin Invest **46**:1318–1328.
5. Dominguez JH, Raisz LG 1979 Effects of changing hydrogen ion, carbonic acid, and bicarbonate concentrations on bone resorption in vitro. Calcif Tissue Int **29**:7–13.
6. Bushinsky DA, Lechleider RJ 1987 Mechanism of proteon-induced bone calcium release: Calcium carbonate dissolution. Am J Physiol **253**:F998–F1005.
7. Bushinsky DA 1988 Net proton influx into bone during metabolic, but not respiratory, acidosis. Am J Physiol **254**: F306–F310.
8. Bushinsky DA 1987 Effects of parathyroid hormone on net proton flux from neonatal mouse calvariae. Am J Physiol **252**:F585–F589.
9. Bushinsky DA, Krieger NS, Geisser DI, Grossman EB, Coe FL 1983 Effects of pH on bone calcium and proton fluxes in vitro. Am J Physiol **245**:F204–F209.
10. Bushinsky DA, Levi-Setti R, Coe FL 1986 Ion microprobe determination of bone surface elements: Effects of reduced medium pH. Am J Physiol **250**:F1090–F1097.
11. Bushinsky DA, Goldring JM, Coe FL 1985 Cellular contribution to pH mediated calcium flux in neonatal mouse calvariae. Am J Physiol **248**:F785–F789.
12. Bushinsky DA 1989 Net calcium efflux from live bone during chronic metabolic, but not respiratory acidosis. Am J Physiol **256**:F836–F842.
13. Chabala JM, Levi-Setti R, Bushinsky DA 1991 Alteration in surface ion composition of cultured bone during metabolic, but not respiratory, acidosis. Am J Physiol **261**:F76–F84.
14. Krieger NS, Sessler NE, Bushinsky DA 1992 Acidosis inhibits osteoblastic and stimulates osteoclastic activity in vitro. Am J Physiol **262**:F442–F448.
15. Bushinsky DA, Sessler NE, Krieger NS 1992 Greater unidirectional calcium efflux from bone during metabolic, than respiratory, acidosis. Am J Physiol **262**:F425–F431.
16. Bushinsky DA 1989 Internal exchanges of hydrogen ions: Bone. In: Seldin DW, Giebisch G (eds.) The Regulation of Acid-Base Balance. Raven Press, New York, pp. 69–88.
17. Bushinsky DA, Krieger NS 1992 Role of the skeleton in calcium homeostasis. In: Seldin DW, Giebisch G (eds.) The Kidney: Physiology and Pathophysiology. Raven Press, New York, pp. 2395–2430.
18. Barzel US 1970 The role of bone in acid base metabolism. In: Barzel US (ed.) Osteoporosis. Grune and Stratton, New York, pp. 199.
19. Bushinsky DA, Chabala J, Levi-Setti R 1989 Ion microprobe analysis of mouse calvariae in vitro: Evidence for a "bone membrane." Am J Physiol **256**:E152–E158.
20. Bushinsky DA, Chabala J, Levi-Setti R 1989 Ion microprobe analysis of bone mineral: Effects of $1,25(OH)_2D_3$. Am J Physiol **257**:E815–E822.
21. Bushinsky DA, Chabala JM, Levi-Setti R 1990 Comparison of in vitro and in vivo $^{44}Ca$ labeling of bone by scanning ion microprobe. Am J Physiol **259**:E586–E592.
22. Krieger NS, Stern PH 1987 Effects of forskolin on bone in organ culture. Am J Physiol **252**:E44–E48.
23. Tashjian AH Jr, Wright DR, Ivey JL, Pont A 1979 Calcitonin binding sites in bone: Relationship to biological response and "escape". Recent Prog Horm Res **34**:285–331.
24. Sprague SM, Bushinsky DA 1990 Mechanism of aluminum-induced calcium efflux from cultured neonatal mouse calvariae. Am J Physiol **258**:F583–F588.
25. Blair NF, Krieger NS, Bushinsky DA 1990 Mechanism of amphotericin-B stimulation of net calcium efflux from bone in vitro. J Bone Miner Res **5**:725–732.
26. Bushinsky DA, Sessler NE 1992 Critical role of bicarbonate in calcium release from bone. Am J Physiol F510–F515.
27. Legeais JM, Hallegot P, Chabala J, Renard G, Levi-Setti R, Galle P 1989 Trifluorothymidine localization in the rat cornea by secondary ion mass spectrometry imaging microanalysis. Curr Eye Res **8**:971–973.
28. Levi-Setti R 1988 Structural and microanalytical imaging of biological materials by scanning microscopy with heavy ion probes. Annu Rev Biophys Biophys Chem **17**:325–347.
29. Levi-Setti R, Crow G, Wang YL 1985 Progress in high resolution scanning ion microscopy and secondary ion mass spectrometry imaging microanalysis. Scanning Electron Microsc **2**:535–551.
30. Levi-Setti R, Wang YL, Crow G 1986 Scanning ion microscopy: Elemental maps at high lateral resolution. Appl Surface Sci **26**:249–264.
31. Linton RW 1986 Biological microanalysis using SIMS—a review. In: Benninghoven A, Colton RJ, Simons DS, Werner HW (eds.) Secondary Ion Mass Spectrometry. Springer, New York, pp. 420–525.
32. Hindie E, Hallegot P, Chabala JM, Thorne NA, Coulomb B, Levi-Setti R, Galle P 1988 Ion microscopy: A new approach for subcellular localization of labeled molecules. Scanning Electron Microsc **2**:1821–1829.
33. Lodding A 1983 Quantitative ion probe microanalysis of biological mineralized tissues. Scanning Electron Microsc **3**: 1229–1242.
34. Vaes G 1988 Cellular biology and biochemical mechanism of bone resorption. A review of recent developments on the formation, activation, and made of action of osteoclasts. Clin Orthop **231**:239–271.
35. Nelson DGA, Featherstone JDB 1982 The preparation, analysis and characterization of carbonated-apatites. Calcif Tiss Int **34**:S69–S81.
36. Bettice JA, Gamble JL Jr 1975 Skeletal buffering of acute metabolic acidosis. Am J Physiol **229**:1618–1624.
37. Swan RC, Pitts RF 1955 Neutralization of infused acid by nephrectomized dogs. J Clin Invest **34**:205–212.
38. Eilon G, Raisz LG 1978 Comparison of the effects of stimulators and inhibitors of resorption on the release of lysosomal enzymes and radioactive calcium from fetal bone in organ culture. Endocrinology **103**:1969–1975.
39. Bushinsky DA 1990 Metabolic acidosis. In: Jacobson HR, Striker GE, Klahr S (eds.) The Principles and Practice of Nephrology. B.C. Decker, Philadelphia, pp. 62–70.
40. Stern PH, Krieger NS 1983 Comparison of fetal rat limb

bones and neonatal mouse calvaria: Effects of parathyroid hormone and 1,25-dihydroxyvitamin $D_3$. Calcif Tissue Int **35**:172–176.

41. Stern PH, Miller JC, Chen SF, Kahn DJ 1978 A bone resorbing substance from bovine serum albumin (brA). Calcif Tissue Res **25**:233–240.

Address reprint requests to:
*David A. Bushinsky, M.D.*
*Professor of Medicine and Physiology*
*University of Rochester School of Medicine and Dentistry*
*601 Elmwood Avenue, Box 675*
*Rochester, NY 14642*

Received in original form March 18, 1992; in revised form July 27, 1992; accepted August 4, 1992.